Ground Penetrating Radar Data Acquisition to Detect Imbalances and Underground Pipes

Tahar Bachiri, Gamil Alsharahi, Abdellatif Khamlichi, Mohammed Bezzazi, and Ahmed Faize

Abstract Past research shows that the Ground Penetrating Radar (GPR) can be an effective and efficient way to map buried pipeline systems. This paper presents a GPR data analysis technique, which is first generated by applying the Finite Differences Time Domain (FDTD) method to estimate the thickness of the subsurface layers and characterize the piping systems buried in the underground. In practical investigations, the GPR unit with a 400 MHz antenna was used to detect imbalances and underground pipes. The GPR profiles provided details on the shapes and nature of the target in the underground. These profiles can, therefore, detect water pipes, utility systems up to a depth than 2 m.

Keywords FDTD method · Ground penetrating radar (GPR) · GPR profiles · Underground pipes

T. Bachiri (✉)
Civil Engineering from Faculty of Sciences and Technology, University Abdelmalek Essaadi, 91001 Tangier, Morocco
e-mail: tbachiri@uae.ac.ma

G. Alsharahi · A. Faize
Department of Physics, Faculty Polydisiplinarly Nador, Mohammed First University, Oujda, Morocco
e-mail: alsharahigamil@gmail.com

A. Faize
e-mail: ahmedfaize6@hotmail.com

A. Khamlichi
Department STIC, National School of Applied Sciences, University Abdelmalek Essaadi, 93030 Tetouan, Morocco
e-mail: khamlichi7@yahoo.es

M. Bezzazi
Department of Mechanical and Civil Engineering, Faculty of Sciences and Technology, University Abdelmalek Essaadi, 91001 Tangier, Morocco
e-mail: bezzazi@hotmail.com

1   Introduction

Today, the underground space, especially in the big cities, is becoming increasingly congested by various networks such as drinking water pipes, telecommunication pipes, gas pipes, liquid sewerage pipes. Spatial information on these underground networks forms the basis of any utility management system. The location of the buried pipe network in the old cities is often unknown. This problem imposes many difficulties when reconstruction takes place in the older parts of a city. Due to the lack of information on the development of underground pipes, for example, civil construction projects can easily damage a hidden pipe and stop the supply of gas or drinking water. It is noted that the operation of underground pipe networks has become a crucial aspect in the field of underground urban engineering [1].

There are several non-destructive methods of detection, such as acoustic detection, electromagnetic induction and GPR [2], which locate underground targets such as buried cables and pipes and monitor water leaks [3–7]. The GPR method is used in many areas of civil engineering and has advantages, including its speed of application, low cost, security, anti-interference, and lack of destruction [8, 9].

This technological tool makes it possible to process all A-scan and B-scan or 2D image waveforms (radargram) by applying a color palette to the reflection intensity values of the recorded electromagnetic waves or amplitudes. In cases, a grayscale color palette is applied, which assigns the black color to the minimum values of electromagnetic wave reflection intensity (minimum amplitude) and the white color at the maximum reflection intensity values of the electromagnetic waves (maximum amplitude). The intermediate values are converted to gray colors of different tone. These B-scans are XZ graphical representations of the reflected electromagnetic waves detected.

2   Principles of Applications GPR in Civil Engineering

GPR has become a more widely used technological tool in the field of civil engineering, particularly its application in the detection of buried pipes. The choice of antennas and the frequency adapted to the situation studied, is fundamental [10, 11]. Most commercially available GPR antennas are bow-tie dipole antennas, with a central frequency fc generally exceeding 400 MHz. Antennas can be divided into types: horn antennas (or aperture) and dipole antennas (or elements). Each antenna has its characteristics and transmit (Tx) and receive (Rx) capability. Also, the low-frequency antennas are physically much larger and transmit a pulse with great penetration into the inspected medium, however, they produce a result with a low resolution of the target under the surface. Civil engineering work involves the measurement of far-field with frequencies often in the frequency range from 400 MHz to 4 GHz, according to this equation:

$$\lambda = \frac{v}{f_c} = \frac{c}{f_c\sqrt{\varepsilon_r'}} \tag{1}$$

where λ is the wavelength of the GPR, fc is the central frequency of the antenna, v is the speed of displacement of the electromagnetic wave in the medium, c is the speed of displacement of the electromagnetic wave in free space, this constant is 0.3 m/ns and ε_r' is the real part of the host material of the complex permittivity. Among the antennas widely used when studying the basic characteristics of an antenna is a short dipole. The antenna diameter and width are minimal compared to the λ length of the radiated wave, so that the excitation current of the antenna is especially uniform along its length. The distance to the far-field boundary can be estimated as follows [12–14]:

$$R_{FF} = \frac{2L_A^2}{\lambda} + \lambda \tag{2}$$

where L_A is a characteristic antenna length and a value of R_{FF} of less than 3 λ is also taken as an overall minimum. Spatial resolution calculation, for a GPR system, is always conditioned by many factors such as frequency, antenna properties, host medium properties and beam angle. The shape of the radiation has a significant influence on the footprint of the GPR beam. The footprint is often calculated as the first Fresnel area (FFA) in the field. The following equation is used for its performance and estimation efficiency [15, 16]:

$$A = \sqrt{\left(\frac{v^2}{16f_c^2} + \frac{vz}{2f_c}\right)} \tag{3}$$

where A is the radius de FFA.

La résolution horizontale Rh de chaque antenne, en fonction d'une distance de 30 cm entre la surface du réflecteur et l'antenne, et la résolution verticale Rv peuvent être estimées comme suit. The horizontal resolution Rh for each antenna based on a distance of 30 cm between the reflector surface and the antenna and the vertical resolution Rv can be estimated as follows [7, 17–19]

$$\left.\begin{array}{l} R_h = 2\left(\frac{\lambda^2}{4} + d\lambda\right)^{\frac{1}{2}} \\ R_v = \frac{1{,}39.v.\Delta t}{2} \end{array}\right\} \tag{4}$$

where d is the vertical distance between the antenna and the reflector surface and Δt is the effective duration of the GPR pulse.

The depth resolution is defined as the minimum distance between two layers so that the latter appears distinct during GPR surveys. The data recorded by the GPR (pulse radar) is based on the sending of an electromagnetic pulse through an antenna on the surface, then the recording of reflected electromagnetic waves from the internal

interfaces, where there is a contrast in dielectric properties. Since the bidirectional travel time measured between Tx and Rx is half the time (ti).

Therefore, the thickness of the third layer can be estimated by the following equation:

$$z_i = \frac{ct_i}{2\sqrt{\epsilon'_r, i}}$$

(5)

Where z_i is the thickness of the ith layer, t_i is the electromagnetic wave travel time through the ith layer.

In order to validate the concept against the GPR techniques for the material distortion of buried pipes, a numerical simulation was carried out using the GprmaxV2.0 software in the Matlab environment.

3 Methodology

The free software GprMax in the Matlab environment [20] was used in the numerical simulation to solve Maxwell equations in the time domain which is based on the FDTD method [21]. This software is simple and robust in electromagnetic modeling and makes it possible to distinguish different sizes of buried targets with various depths in different mediums, such as free space, water, sand, clay, concrete. GprMax input file that includes all the information to run a model requires information about materials, geometry, antenna, and other features to perform the simulation. A 2D model is chosen to perform B-scan perpendicular on pipes of different types such as cast iron, plastic, and concrete. Each pipe has a diameter of 100 mm and is buried inhomogeneous concrete-covered soil at a depth of 20.4 cm. The model geometry is illustrated in Fig. 1.
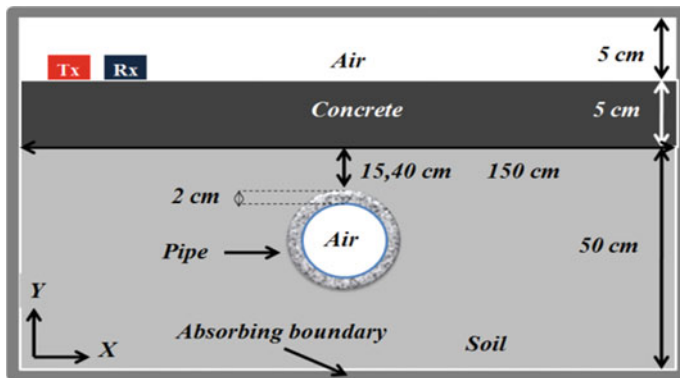

Fig. 1 Model geometry of pipe in soil recovered with concrete

Table 1 GPR model description

|		Permeability μ_r	Permittivity ε_r'	Conductivity σ(S/m)
Medium	Concrete	1	6	10^{-3}
	Soil	1	9	10^{-3}
Materials of pipe	Concrete with air	1	6	10^{-3}
	Plastic with air	1	3	10^{-4}
	Void with water	1	81	5×10^{-4}
	Metal with air	Perfect conductor		
Geomtry models		domain: 1.30 0.6		
		dx_dy: 0.005 0.005 m		
		Time_window: 12.0e−9 s		
Antenna (Tx/Rx)		Scanning: Axis X		
		Offset (Tx/Rx): 13 cm		
		Source type: Ricker		
		Frequency: 400 MHz		

Table 1 lists the description of the GPR model with the antenna parameters and medium geometry.

4 Results and Discussion

4.1 Numerical Simulations

The simulated GPR data was performed by placing the GPR on the target and moving the coil along an X-axis and perpendicular to the pipe. Figure 2 shows the A-scan measurements of the tube center position, while Fig. 3 shows the parabolic signatures that appear on the GPR radargram.

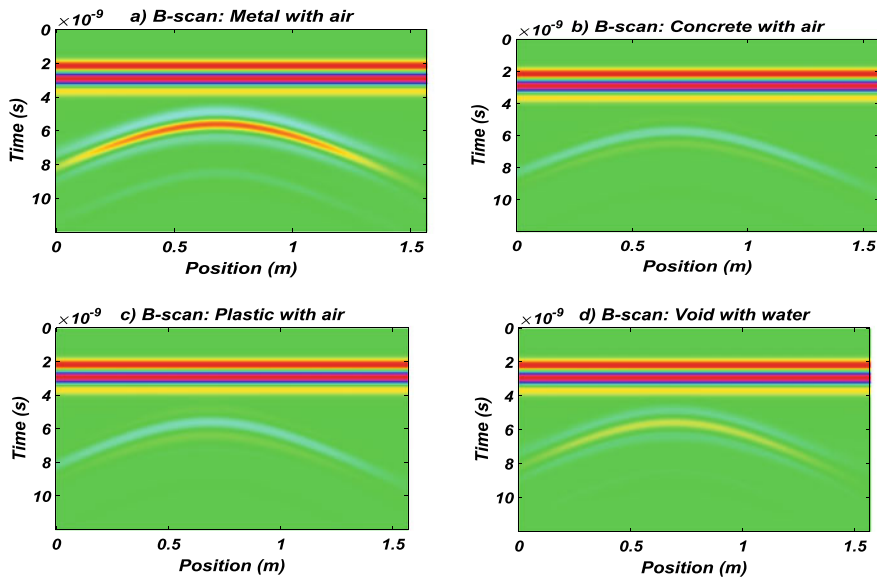**Fig. 2** A-scan for detecting an empty pipe
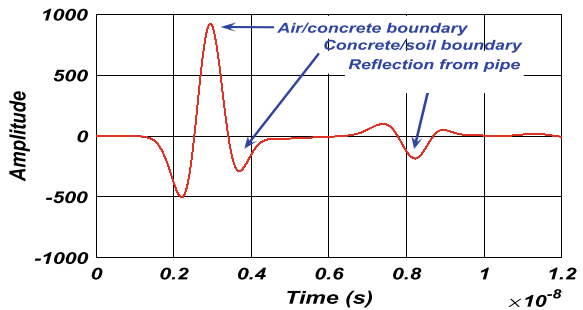
Fig. 3 Model and GPR images with different materials of pipe constructed at same color scale:
a air-filled metal pipe, **b** air-filled concrete pipe, **c** air-filled plastic pipe, **d** water-filled vacuum

Based on Fig. 2, the distances from the GPR antenna to the air/concrete interface, to the concrete/soil interface and the upper generator interface of the pipe, can be estimated using the differential travel times of the antenna at these interfaces. The thickness of the concrete layer and the depth of burial of the pipe can be determined respectively by multiplying the speed of the electromagnetic wave in the concrete and the ground and the differential travel times of the electromagnetic wave between the interfaces sus-indicated. Using the example in Fig. 2, the travel time between the two air/concrete and concrete/ground interfaces is 0.785 ns and the travel time between the concrete/ground interfaces and the top pipe generator is 2.97 ns. Using Eq. (5), we can estimate the thickness of the concrete layer is 4.807 cm with a 3.86% error percentage and that the depth of the pipe is 19.657 cm with a 3.64% error percentage.

The B-scans of the numerical simulations are shown in Fig. 3. These results illustrate the distinction between pipes that are made up of different materials in a medium that includes two layers of concrete ($\varepsilon'_r = 6$) and soil ($\varepsilon'_r = 9$). These simulations show good resolution while simultaneously solving the location of the pipes with good precision. Based on the resolution properties, it may be suggested that GPR with a central frequency of 400 MHz is suitable for providing indirect information on the nature of buried pipe materials.

The most significant feature observed is when the nature of the pipe materials changes, the intensity of the hyperbole function also changes. For example, the B-scan simulating a metal pipe (a) has clear contrasts with other acquisitions (b–d), because the difference in dielectric constant between steel and ground is the greater of

the three conditions, and the reflection of the electromagnetic wave is stronger. In the B-scans (b, c) of the empty pipes, there is a double reflection of the electromagnetic wave, because the second reflected curve comes from the lower edge of the pipe. Since water strongly absorbs the electromagnetic wave, only one electromagnetic wave curve can be seen in the B-scan (d) relating to an empty opening filled with water. Note that all these B-scans are done on the same color scale. Similar results were obtained in [22–25].

It can be argued that B-scan observations are unavoidable due to the high contrast between the host medium and the permittivity of pipe materials. To mount this, we note the decrease in the intensity of hyperbolic reflections is always present with low permittivity pipe materials. The ability to obtain acceptable resolution B-scans with a 400 MHz GPR that is capable of clearly distinguishing the nature of pipe materials, is possible in conventional GPR surveys as prescribed in this paper.

4.2 Practical Application

GPR profiles using 400 MHz antennas were acquired at the site. First, the acquisition of GPR data was performed on known targets, to allow the calibration of GPR equipment. We then carried out on-site GPR profiles to cover the entire zone to be examined. GPR processing was done by the Radan software, using standard steps such as zero-time correction and the application of a band-pass filter. The physical parameters that are taken as a function of medium moisture are relative dielectric permittivity ($\varepsilon_r = 9$) and electrical conductivity ($\sigma = 0.001$ s/m). Among the many GPR profiles that have been acquired in the site, we present in this paper only the most representative ones. In addition to the GPR profiles, we did a full scan of the area with the VIVAX VLOC Pro2 brand radio detector, which allows us to detect buried arrays at quite significant depths compared to the GPR up to 5 m or more when using the detector in active mode. On the different profiles we observe:

On the GPR image below (Fig. 4) we see the presence of reinforcements in the concrete with a rather high reinforcement density. There is also heterogeneity of the subsoil, in the form of a clear hyperbolic reflection of low amplitude, which is located at the position up to 4.40 m and a depth bounded between 0.60 m and 1.40 m because this does not repeat on the other profiles. A view of the perpendicular profiles made in this area, confirms the presence of an object in the basement.

The existence of a reinforced concrete slab prevents penetration of the reflected GPR signal back to the surface. This signal can be reflected again and re-enters the basement, causing a reverberation signal, masking information from deeper depths.

Hyperbolic reflections are observed in Fig. 5 corresponding to five pipes, which are placed next to each other, used to transport stormwater. These pipes are confirmed at the same depth of 2.20 m from the top pipe generator.

In Fig. 6 the measurement was carried out on a full drinking water pipe located on the subsurface; it can be seen that the rate of propagation of electromagnetic waves decreases due to high relative permittivity ($\varepsilon'_r = 81$). The delay of the reflected
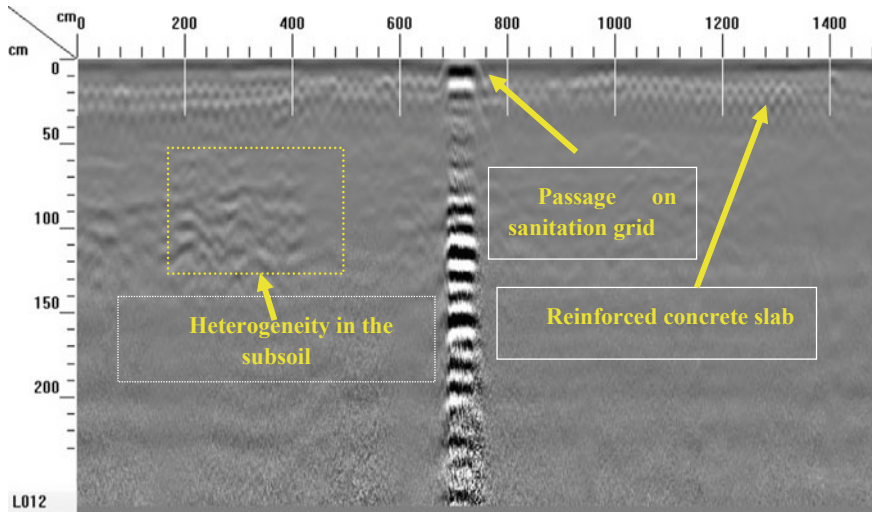
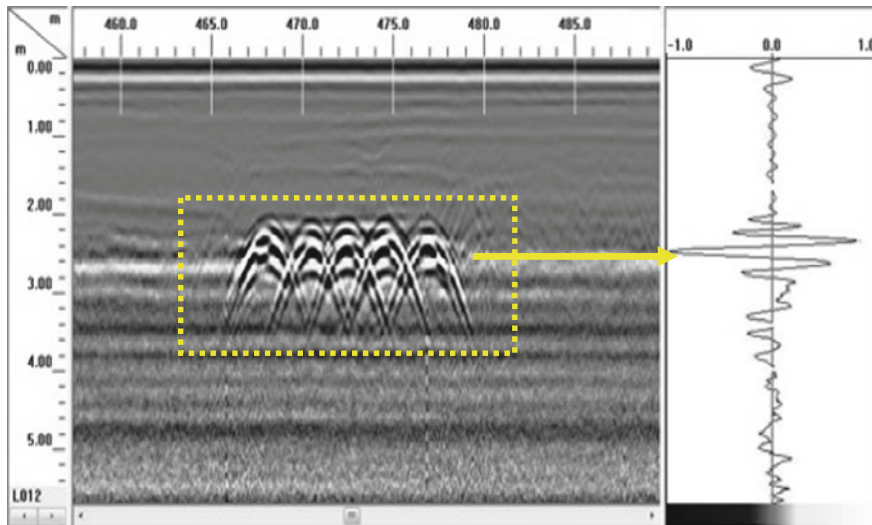Fig. 4 GPR profile showing reinforced concrete slab and subsoil heterogeneity

Fig. 5 GPR profile shows five metal pipes that are located at the same depth

wave which is recorded by the receiving antenna generates, at different times, the hyperboles corresponding to the reflections of electromagnetic waves.

In Fig. 7a, we see two sewer pipes clogged by waste. These two pipes are confirmed from a depth of 2 m and are approximately 0.50 m above each other. In the profile associated to Fig. 7b, clear hyperbolic forms are observed, it is a single pipe that
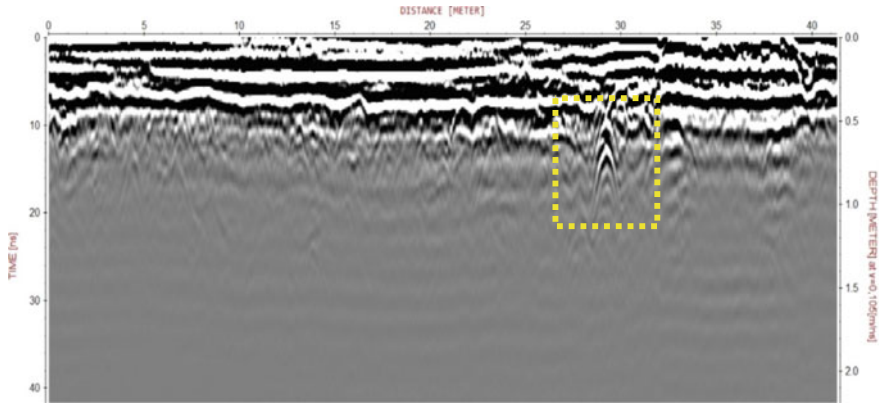
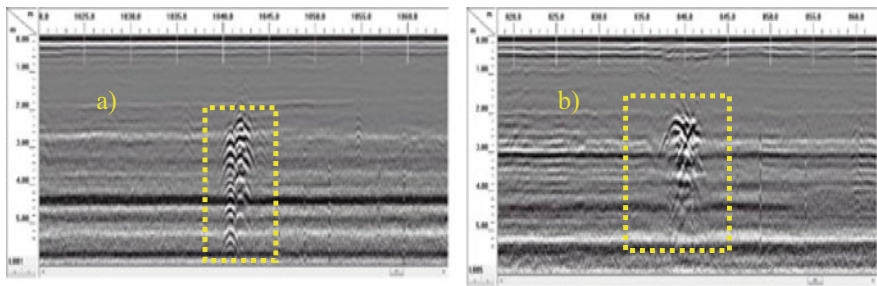**Fig. 6** GPR profile shows a water-filled pipe on the subsurface

Fig. 7 a, **b** Radargrams of the profiles detecting sewer pipes

shows an imbalance. This pipe can be broken and filled with alluvial and clay-silty sediments. The hyperboles were obtained with a peak of 2.10 m.

This study shows that the GPR method is an important step before starting civil works, because it provides the precise location of utilities in the underground, as well as an estimate of their depths. Based on these results, interventions to remedy anomalies accurately, safely and without risk of dangerous accidents. The information improves and updates public service placement plans and serves as a basis for urban planning. This paper complements the work already published in [7].

5 Conclusions

This paper has been carried out to develop the use of GPR techniques in the field of civil engineering, in particular the assessment of the condition and defects of pipeline networks. The numerical simulation can provide a solid database of data from the underground, which allows a concrete validation of the principle for the use of the

GPR technique with a 400 MHz antenna (Tx) that is suitable for this type of survey evaluation.

In practical investigations, despite the presence of a reinforced concrete slab, which could have attenuated the GPR signal, we were able to detect an anomaly that is related to a heterogeneity of the ground. The GPR profiles provided details on the shapes and nature of the target in the basement. These profiles can, therefore, detect water pipes, utility systems in the basement up to a depth of than 2 m.

References

1. Costello SB, Chapman DN, Rogers CDF, Metje N (2007) Underground asset location and condition assessment technologies. Tunnel Underground Space Technol 22(5–6):524–542
2. Daniels DJ (2004) Ground penetrating radar, 2nd edn. Institution of Electrical Engineers, London
3. Zeng X, McMechan GA (1997) GPR characterization of buried tanks and pipes. Geophysics 62(3):797–806
4. Pettinelli E, Di Matteo A, Mattei E, Crocco L, Soldovieri F, Redman JD, Annan AP (2009) GPR response from buried pipes: Measurement on field site and tomographic reconstructions. IEEE Trans Geosci Remote Sens 47(8):2639–2645
5. Ristić A, Bugarinović Ž, Govedarica M, Pajewski L, Derobert X (2017) Verification of algorithm for point extraction from hyperbolic reflections in GPR data. In: 2017 9th international workshop on advanced ground penetrating radar (IWAGPR). IEEE, pp 1–5
6. Ghorbel O, Ayadi A, Ayadi R, Aseeri M, Abid M (2019) Combined methods based outlier detection for water pipeline in wireless sensor networks. In: International conference on advanced information networking and applications. Springer, Cham, pp 214–224
7. Bachiri T, Alsharahi G, Khamlichi A, Bezzazi M, Faize A (2020) GPR application in civil engineering to search and detect underground Networks. Int J Emerg Trends Eng Res 8(5). https://www.warse.org/IJETER/static/pdf/file/ijeter59852020.pdf
8. Benedetto A, Pajewski L (2015) Civil engineering applications of ground penetrating radar. Trans Civ Environ Eng
9. Faize A, Alsharahi G (2020) Preliminary study of roots by georadar system. In: Embedded systems and artificial intelligence. Springer, Singapore, pp 173–182
10. Bachiri T, Khamlichi A, Bezzazi M (2018) Detection of rebar corrosion in bridge deck by using GPR. In: MATEC web of conferences, vol 191. EDP Sciences, p 00009
11. Tosti F, Ferrante C (2019) Using ground penetrating radar methods to investigate reinforced concrete structures. Surv Geophys 2019:1–46
12. Yaghjian A (1986) An overview of near-field antenna measurements. IEEE Trans Antennas Propag 34(1):30–45
13. Millard SG, Shaari A, Bungey JH (2002) Field pattern characteristics of GPR antennas. NDT & E Int 35(7):473–482
14. Van der Wielen A, Courard L, Nguyen F (2012) Detection of thin layers into concrete with static and CMP measurements. In: 2012 14th international conference on ground penetrating radar (GPR). IEEE, pp 530–535
15. Pérez-Gracia V, González-Drigo R, Di Capua D (2008) Horizontal resolution in a non-destructive shallow GPR survey: an experimental evaluation. NDT E Int 41(8):611–620
16. Luo TX, Lai WW (2020) GPR pattern recognition of shallow subsurface air voids. Tunnel Underground Space Technol 99:103355
17. Jol HM (2009) Ground penetrating radar: theory and applications. Elsevier Sciences
18. Pérez-Gracia V, Di Capua D, González-Drigo R, Pujades L (2009) Laboratory characterization of a GPR antenna for high-resolution testing: radiation pattern and vertical resolution. NDT & E Int 42(4):336–344

19. Prego FJ, Solla M, Puente I, Arias P (2017) Efficient GPR data acquisition to detect underground pipes. NDT & E Int 91:22–31
20. Giannopoulos A (2005) Modelling ground penetrating radar by GprMax. Constr Build Mater 19(10):755–762
21. Kunz KS, Luebbers RJ (1993) The finite difference time domain method for electromagnetics. CRC Press
22. Alsharahi G, Faize A, Maftei C, Bayjja M, Louzazni M, Driouach A, Khamlichi A (2019) Analysis and modeling of GPR signals to detect cavities: case studies in Morocco. J Electromagnet Eng Sci 19(3):177–187
23. Prego FJ, Solla M, Puente I, Arias P (2017) Efficient GPR data acquisition to detect underground pipes. NDT E Int 91:22–31
24. Alsharahi G, Faize A, Louzazni M, Mostapha AMM, Bayjja M, Driouach A (2019) Detection of cavities and fragile areas by numerical methods and GPR application. J Appl Geophys 164:225–236
25. Alsharahi G, Mint Mohamed Mostapha A (2016) Modelling and simulation resolution of ground penetrating radar antennas. J Electromagnet Eng Sci